CHIN. PHYS. LETT. Vol. 33, No. 12 (2016) 128103

Molecular Beam Epitaxy of Zero Lattice-Mismatch InAs/GaSb Type-Ⅱ Superlattice *

Hai-Long Yu(于海龙), Hao-Yue Wu(吴皓越), Hai-Jun Zhu(朱海军), Guo-Feng Song(宋国峰), Yun Xu(徐云)**

Nano-Optoelectronics Laboratory, Institute of Semiconductors, Chinese Academy of Sciences, BeiJing 100083

(Received 8 August 2016)

Type-Ⅱ InAs/GaSb superlattices made of 13 InAs monolayers (MLs) and 7 GaSb MLs are grown on GaSb substrates by solid source molecular beam epitaxy. To obtain lattice-matched structures, thin InSb layers are inserted between InAs and GaSb layers. We complete a series of experiments to investigate the influence of the InSb deposition time, V/Ⅲ beam-equivalent pressure ratio and interruption time between each layer, and then characterize the superlattice (SL) structures with high-resolution x-ray diffraction and atomic force microscopy. The optimized growth parameters are applied to grow the 100-period SL structure, resulting in the full-width half-maximum of 29.55 arcsec for the first SL satellite peak and zero lattice-mismatch between the zero-order SL peak and the GaSb substrate peak.

PACS: 81.05.Ea, 81.10.Pq, 74.78.Fk, 81.15.−z DOI: 10.1088/0256-307X/33/12/128103

First proposed by Smith *et al.*[1] in 1987, type-Ⅱ InAs/GaSb superlattices (SLs) have garnered considerable interests from researchers and developers as a promising material system for infrared detection.[2–4] One of the main advantages of this material system is that its effective bandgap can be tailored over a wide range (3–30 μm) by varying the thicknesses of InAs and GaSb.[5–12] Although the SLs system was proposed over a decade ago, the performances of InAs/GaSb superlattices infrared detectors have not yet reached their theoretical prediction and remain inferior to HgCdTe. One important issue that limits superlattices detector performances is the quality of the material.[7] Therefore, it is desirable to grow high-quality superlattice materials for applications in infrared devices.

Even though the lattice mismatch between InAs and GaSb is as low as 0.6%, the multi-layered nature of the superlattices results in undesirable accumulative tensile strain. InSb interface formation is commonly applied[13,14] between the superlattice layers to compensate for this structure strain. The strain-balancing contribution of the InSb inserted layer improves the SL quality while it also allows total active zone thickness up to several micrometers,[15] which facilitates high optical absorption efficiency. However, due to the large lattice mismatch (>6%) between InSb and GaSb layers, the island growth mode is easily caused. Although the growth of the SL structures with InSb inserted layers has been widely researched,[16–19] few have obtained zero lattice-mismatch. In this study, we investigate the molecular beam epitaxy and characterization of 100-period InAs/GaSb type-Ⅱ superlattice structures designed for long wavelength infrared detectors. We focus especially on controlling the InSb inserted layer, V/Ⅲ beam-equivalent pressure (BEP) ratio and interruption time between each layer. The structural quality of material is examined via high-resolution x-ray diffraction (HRXRD) and surface morphology is assessed by atomic force microscopy (AFM). Lastly, zero lattice-mismatch InAs/GaSb type-Ⅱ superlattices is obtained with inserted InSb layers.

We grew our samples on epi-ready GaSb substrates by a Riber412 molecular beam epitaxy system equipped with valved arsenic (As) and antimony (Sb) cracker cells. Dual-filament effusion cells were used for gallium (Ga) and indium (In). All the SL structures in this study contained 100 periods and 13 ML InAs/7 ML GaSb per period. The thin InSb layer was inserted between InAs and GaSb. Different interruption times were introduced between each layer. Growth rates were 0.5 ML/s for GaSb and 0.38 ML/s for InAs. The background pressure of the growth chamber maintained in the low 10^{-10} torr. Growth temperatures reported here are pyrometer reading referenced to the GaSb oxide desorption temperature of 530℃. After the buffer layer growth, the temperature was lowered down to 405℃ to grow SLs structures. The beam equivalent pressures (BEP) of the molecular fluxes were measured by using an ionization gauge during each sample growth. The V/Ⅲ BEP ratios were 4 for InAs and 3.6 for GaSb, respectively.

Four samples in set A were grown with different InSb thicknesses, varying from 0.4 ML to 0.7 ML, to determine the effect of the InSb thickness on strain. The FWHM for the first-order peak of SLs and the

*Supported by the National Basic Research Program of China under Grant Nos 2015CB351902, 2015CB932402 and 2012CB619203, the National Natural Science Foundation of China under Grant Nos 61177070, 11374295 and U1431231, and the National Key Research Program of China under Grant No 2011ZX01015-001.

**Corresponding author. Email: xuyun@semi.ac.cn

© 2016 Chinese Physical Society and IOP Publishing Ltd

lattice mismatch between the zero-order peak of the SLs and GaSb substrate are calculated for set A (Fig. 1(a)). With presence of 0.64 ML InSb thickness, the lattice mismatch and FWHM of the first-order SL peak are improved compared with other samples (reaching 0 ppm and 29.55 arcsec, respectively). However, as the InSb layer thickness further increases, the SLs lose their structural quality. We attribute this degradation to a possible change in growth mode from layer-by-layer to 3D island formation. The HRXRD curves of the SL layers containing different InSb thicknesses are shown in Fig. 2. The zero-order peak position of the SLs moves from right to left of the GaSb substrate diffraction peak as the InSb thickness increases, reflecting the increase in the SL lattice constant. The HRXRD result shows that the zero-order satellite peak coincides with the GaSb substrate peak, as shown in Fig. 2(c), implying that the lattice mismatch is zero.

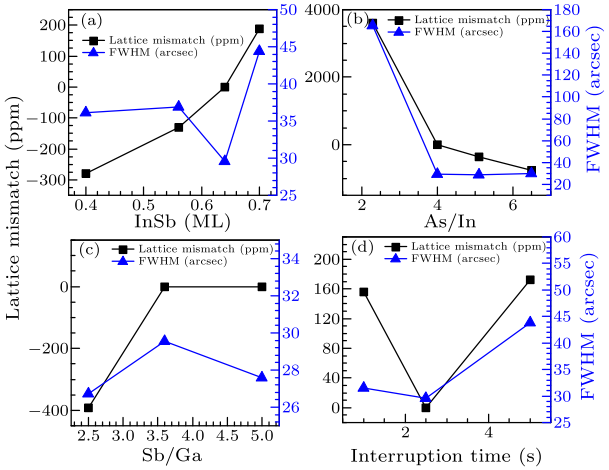

Fig. 1. FWHM of the first-order SLs peak and lattice mismatch between the zero-order SLs peak and the GaSb substrate for (a) InSb thickness, (b) As/In flux ratio, (c) Sb/Ga flux ratio and (d) interruption time between each layer.

Set B includes four samples grown with different As/In flux ratios from 2.3 to 6.5. The first-order FWHM and the lattice mismatch are shown in Fig. 1(b) as a function of the As/In flux ratio. We change the As/In flux ratio only by different As fluxes. It can be seen from the figure that zero lattice mismatch can be obtained at an As/In flux ratio of 4. When the As/In flux ratio decreases from 4 to 2.3, the lattice mismatch and the FWHM value increase dramatically from 0 ppm to 3608 ppm and from 29.55 arcsec to 165.5 arcsec, respectively. When the As/In flux ratio increases from 4 to 5.1 and 6.5, the residual As atoms will mix into InSb and GaSb layers, which results in that a part of the original layers will transform into $InAs_{1-x}Sb_x$ and $GaAs_{1-x}Sb_x$. The average lattice constant of SLs with larger As/In flux ratio become smaller because the lattice constants of $InAs_{1-x}Sb_x$ and $GaAs_{1-x}Sb_x$ are smaller than InSb and GaSb, respectively. This is the reason that lattice mismatch of the sample with larger As/In flux ratio is a negative value. The As valve was screwed down to 0% during growth of GaSb layers, to make residual As the lowest level in the growth chamber. The negative value of lattice mismatch illustrates that even the As valve was screwed down to 0% in growth of InSb and GaSb layers, there were still many residual As atoms mixed into other layers, resulting in SLs needing more InSb inserted to provide strain balance. In a previous study,[14,20–22] researchers reported that SL material quality would be degraded significantly when the InSb layer was inserted more than one monolayer due to the possible change in growth mode from layer-by-layer to 3D island formation. To avoid this degradation, we must control the As flux large enough to obtain good InAs quality and small enough to avoid overmuch As mixing into other layers.

Set C includes three samples grown with different Sb/Ga flux ratios. We change the Sb/Ga flux ratio only with different Sb fluxes. The first-order FWHM and lattice mismatch are shown in Fig. 1(c) as a function of the Sb/Ga flux ratio. When the Sb/Ga flux ratio decreases from 3.6 to 2.5, the lattice mismatch increases significantly from 0 ppm to −392.6 ppm. When the Sb/Ga flux ratio becomes larger (from 3.6 to 5), the lattice mismatch can be kept at zero value invariant. According to our experience, the vacuum of the growth chamber is a lower order of magnitude when Sb flux is the same as As flux. It means that, compared with As atoms, Sb atoms are not easily incorporated into the InAs layer due to their characteristics of diffusion. This is the reason that lattice mismatch keeps invariant when the Sb/Ga flux ratio becomes larger while lattice mismatch turns to a negative value when the As/In flux ratio increases.

Set D includes three samples grown with different interruption times. The FWHM for the first-order peak of SLs as well as the lattice mismatch between the zero-order peak of SLs and GaSb substrate are calculated for set D and present in Fig. 1(d). With 2.5 s interruption time between InSb and other layers, we obtain the lowest value of lattice mismatch. The lattice mismatch keeps increasing although the interruption time increases from 2.5 to 5 or decreases to 1.

One sample grown with the optimized growth parameters reaches the FWHM of 29.55 arcsec for the first SL satellite peak and zero lattice-mismatch between the zero-order SL peak and the GaSb substrate peak. To verify the superlattice material quality, we assess its surface morphology by AFM. The AFM image on a $2\,\mu m \times 2\mu m$ scan area is shown in Fig. 3.

The rms surface roughness is 0.255 nm, illustrating that the surface morphology is quite good, compared with reports from other groups. Figure 4 depicts the PL spectra of the sample measured at 77 K. In spite of the fact that the period of the SLs is only 100, a clear PL signal is observed. The PL peak position is about 9.15 μm.

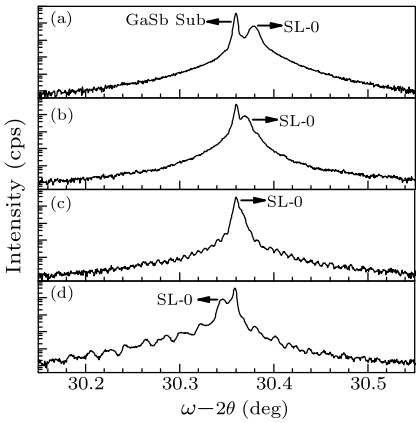

Fig. 2. HRXRD curves for set A samples containing different InSb thicknesses: (a) 0.4 ML, (b) 0.56 ML, (c) 0.64 ML, (d) 0.7 ML.

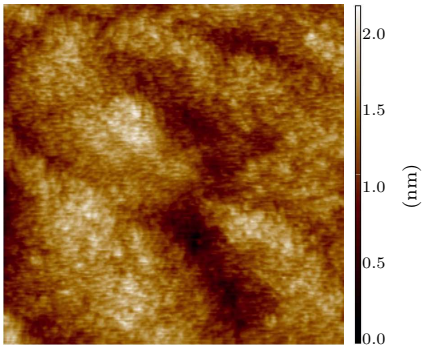

Fig. 3. AFM cartography of a 2 μm×2μm scan area for the sample grown with the optimized growth parameters.

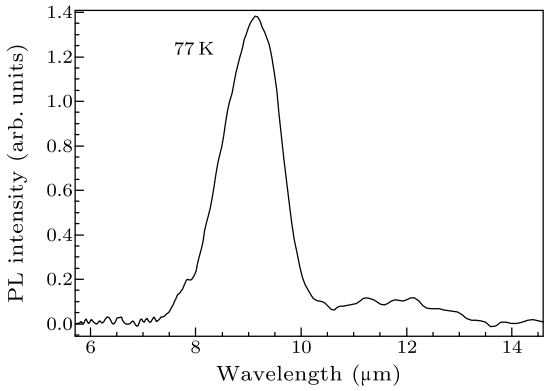

Fig. 4. Photoluminescence spectra of the SL structures with 100 periods measured at 77 K.

Finally, the p–i–n SL structure was grown to verify the superlattices material quality with our growth method and parameters. The growth sequence includes a 500 nm p^+-GaSb bottom layer, 500 periods of SLs and a 20 nm n^+-InAs top contact layer. The SL region consists of 100-period p-type, 300-period undoped and 100-period n-type InAs/GaSb SL layers. The HRXRD measurement curve of the p–i–n structure shows sharp satellite peaks up to 4th order, as shown in Fig. 5. The FWHM of the first-order peak is 35 arcsec. The HRXRD result shows that the zero-order satellite peak coincides with the GaSb substrate peak, as shown in the inset of Fig. 5, implying that the lattice mismatch is zero. The small FWHM value as well as the high order of well-defined satellite peaks and their very periodic arrangement indicate the excellent crystal quality of the layers.

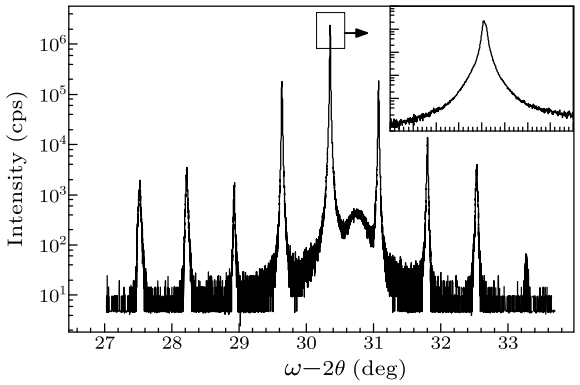

Fig. 5. The HRXRD curve of the p–i–n photodetector grown with the optimized SLs.

In summary, long-wave infrared type-Ⅱ InAs/GaSb superlattices, including inserted InSb layers between InAs and GaSb layers to achieve strain compensation to GaSb substrates, have been grown by solid source molecular beam epitaxy. High-quality strain-balanced SL structures of 13 InAs MLs/7 GaSb MLs are obtained. We systematically investigate the influence of the InSb inserted layer thickness, V/Ⅲ flux ratio and interruption time between growing layers, then characterize the SL structures with HRXRD and AFM. With the 0.64 ML InSb layer and 2.5 s interruption time between InSb inserted layers and other layers, we obtain a FWHM of 29.55 arcsec of the first-order satellite peak and zero lattice mismatch between the zero-order satellite SLs peak and the GaSb substrate peak.

References

[1] Simth D L and Mailhiot C 1987 *J. Appl. Phys.* **62** 2545
[2] Nguyen B M, Hoffman D, Wei Y et al 2007 *Appl. Phys. Lett.* **90** 231108
[3] Wei Y, Hood A, Yau H, Yazdanpanah V et al 2005 *Appl. Phys. Lett.* **86** 091109
[4] Plis E, Rodriguez J B, Kim H S, Bishop G et al 2007 *Appl. Phys. Lett.* **91** 133512
[5] Walther M, Schmitz J, Rehm R, Kopta S et al 2005 *J. Cryst. Growth* **278** 156

[6] Chen J X, Zhou Y, Xu Z C et al 2013 *J. Cryst. Growth* **378** 596
[7] Rhiger D R, Kvaas R E, Harris S F, Bornfreund R E et al 2007 *Proc. SPIE* **6542** 654202
[8] Chen J X, Xu Q Q, Zhou Y et al 2011 *Nanoscale Res. Lett.* **6** 635
[9] Satpati B, Rodriguez J B, Trampert A et al 2007 *J. Cryst. Growth* **301** 889
[10] Khoshakhlagh A, Plis E, Myers S and Sharma Y D 2009 *J. Cryst. Growth* **311** 1901
[11] Haugan H J, Brown G L and Grazulis L 2011 *J. Vac. Sci. Technol.* B **29** 03C101
[12] Arikan B, Korkmaz M, Aslan B and Serincan U 2015 *Thin Solid Films* **589** 813
[13] Rodriquez J B, Christol P, Cerutti L and Chevrier F 2005 *J. Cryst. Growth* **274** 6
[14] Haugan H J, Grazulis L, Brown G J, Mahalingam K et al 2004 *J. Cryst. Growth* **261** 471
[15] Plis E, Annamalai S and Posani K T 2006 *J. Appl. Phys.* **100** 014510
[16] Zhang Y H, Ma W Q, Cao Y L and Huang J L 2011 *IEEE J. Quantum Electron.* **47** 1475
[17] Arikan B, Korkmaz G and Suyolcu Y E 2013 *Thin Solid Films* **548** 288
[18] Tahraoui A, Tomasini P, Lassabatere L et al 2000 *Appl. Surf. Sci.* **162** 425
[19] Kaspi R, Steinshnider J, M Weimer et al 2001 *J. Cryst. Growth* **225** 544
[20] Wen L, Gao F L, Zhang X N, Zhang S G et al 2014 *J. Appl. Phys.* **116** 193508
[21] Gao F L, Wen L, Zhang S G, Li J L et al 2015 *Thin Solid Films* **597** 25
[22] Bulent A and Melih K 2016 *Appl. Surf. Sci.* **362** 244